

4

TECHNICAL REPORT 17

AD-A225 860

To

The Office of Naval Research
Contract No. N00014-86-K-0381

DTIC
ELECTE
AUG 27 1990
S B D
Co

MICROSTRUCTURAL EVOLUTION IN RAPIDLY
SOLIDIFIED Cu-Nb POWDERS

K. L. Zeik, I. E. Anderson, P. R. Howell, and D. A. Koss

Department of Materials Science and Engineering
The Pennsylvania State University
University Park, PA 16802

Reproduction in Whole or in Part is Permitted
For Any Purpose of the United States Government
Distribution of this Document is Unlimited

90 08 27 380

REPORT DOCUMENTATION PAGE

Form Approved
OMB No. 0704-0188

1a REPORT SECURITY CLASSIFICATION Unclassified		1b RESTRICTIVE MARKINGS	
2a SECURITY CLASSIFICATION AUTHORITY		3 DISTRIBUTION/AVAILABILITY OF REPORT Distribution of this document is unlimited	
2b DECLASSIFICATION/DOWNGRADING SCHEDULE			
4 PERFORMING ORGANIZATION REPORT NUMBER(S) Report No. 17		5 MONITORING ORGANIZATION REPORT NUMBER(S)	
6a NAME OF PERFORMING ORGANIZATION The Pennsylvania State Univ.	6b OFFICE SYMBOL (if applicable)	7a NAME OF MONITORING ORGANIZATION	
6c ADDRESS (City, State, and ZIP Code) Dept. of Materials Science & Engineering The Pennsylvania State University University Park, PA 16802		7b ADDRESS (City, State, and ZIP Code)	
8a NAME OF FUNDING/SPONSORING ORGANIZATION Office of Naval Research	8b OFFICE SYMBOL (if applicable)	9 PROCUREMENT INSTRUMENT IDENTIFICATION NUMBER N00014-86-K-0381	
8c ADDRESS (City, State, and ZIP Code) Office of Naval Research, Code 1131 800 N. Quincy Street Arlington, VA 22217		10 SOURCE OF FUNDING NUMBERS	
		PROGRAM ELEMENT NO	PROJECT NO
		TASK NO	WORK UNIT ACCESSION NO.
11 TITLE (Include Security Classification) Microstructural Evolution in Rapidly Solidified Cu-Nb Powders			
12 PERSONAL AUTHOR(S) K. L. Zeik, I. E. Anderson, P. R. Howell and D. A. Koss			
13a. TYPE OF REPORT	13b TIME COVERED FROM _____ TO _____	14 DATE OF REPORT (Year, Month, Day) August 22, 1990	15 PAGE COUNT 27
16 SUPPLEMENTARY NOTATION			
17 COSATI CODES		18 SUBJECT TERMS (Continue on reverse if necessary and identify by block number)	
FIELD	GROUP	SUB-GROUP	
			Gas Atomization Undercooling
			Rapid Solidification Cooling Rate,
			Cu-Nb Alloys Microstructure.
19 ABSTRACT (Continue on reverse if necessary and identify by block number) High pressure inert gas atomization has been used to produce rapidly solidified Cu-21.2wt%Nb powders with a range of particle sizes and microstructures. The associated microstructures depend on particle size. Specifically, fine-scale particles (<15 μm) are characterized by a predominance of Nb-rich, multiphase spheroids and a small population of nearly pure Nb dendrites in an almost pure matrix of Cu. In contrast, large particles (45-75 μm) contain only Nb dendrites in a Cu matrix. The volume fraction of "second phase" is much lower in the latter instance than in the former. The change in microstructure with particle size is believed to be a result of both the amount of undercooling and cooling rate of the liquid droplets prior to and during solidification. In particular, the large undercoolings in the fine particles are believed to induce a non-equilibrium liquid phase separation which results in a high volume fraction of spheroidal, multiphase Nb-Cu particles within a Cu-rich matrix containing Nb dendrites.			
20 DISTRIBUTION/AVAILABILITY OF ABSTRACT <input type="checkbox"/> UNCLASSIFIED UNLIMITED <input checked="" type="checkbox"/> SAME AS RPT <input type="checkbox"/> DTIC USERS		21 ABSTRACT SECURITY CLASSIFICATION Unclassified	
22a NAME OF RESPONSIBLE INDIVIDUAL Donald A. Koss		22b TELEPHONE (Include Area Code) 814-865-5447	22c OFFICE SYMBOL

MICROSTRUCTURAL EVOLUTION IN RAPIDLY SOLIDIFIED Cu-Nb POWDERS

K. L. ZEIK¹, I. E. ANDERSON², P. R. HOWELL¹, & D. A. KOSS¹.

¹ Department of Materials Science and Engineering
Pennsylvania State University, University Park, PA 16802

² Ames Laboratory, Iowa State University, Ames, IA 50011

Abstract

High pressure inert gas atomization (HPGA) has been used to produce rapidly solidified Cu-21.2wt%Nb powders with a range of particle sizes and microstructures. The associated microstructures depend on particle size. Specifically, fine-scale particles (<15 μm) are characterized by a predominance of Nb-rich, multiphase spheroids and a small population of nearly pure Nb dendrites in an almost pure matrix of Cu. In contrast, large particles (45-75 μm) contain only Nb dendrites in a Cu matrix. The volume fraction of "second phase" is much lower in the latter instance than in the former. The change in microstructure with particle size is believed to be a result of both the amount of undercooling and cooling rate of the liquid droplets prior to and during solidification. In particular, the large undercoolings in the fine particles are believed to induce a non-equilibrium liquid phase separation which results in a high volume fraction of spheroidal, multiphase Nb-Cu particles within a Cu-rich matrix containing Nb dendrites.

<input checked="" type="checkbox"/>
<input type="checkbox"/>
<input type="checkbox"/>



Distribution/	
Availability Codes	
Dist	Avail and/or Special
A-1	

1. Introduction

The copper-niobium alloy system has been of considerable interest as a basis for fabrication of superconducting materials in the form of cast and drawn fine wires [1,2]. Research on these materials led to the discovery that the Cu-Nb wires exhibited anomalously high strengths, exceeding that predicted by a rule of mixtures analysis [3-5]. The extensive mechanical reductions of cast microstructures, characterized by random arrays of niobium dendrites dispersed within a continuous copper matrix, caused the formation of an aligned, filamentary "in-situ" composite. The size and spacing of the aligned, discontinuous niobium filaments was found to determine the strength [5]. It was subsequently shown that the size and spacing of the niobium filaments were dependent on the scale of the original cast microstructure. Thus, techniques which could produce an enhanced refinement of the dispersed second phase in the initial solidified microstructure could also lead to improved mechanical properties with a reduced level of deformation processing [6].

Powder metallurgy (PM) techniques for producing copper-niobium alloys have emerged recently with the potential to generate niobium dispersions which are much finer than those produced by conventional chill casting. For example, mechanical alloying of blended Cu and Nb powders has been used to produce a particulate composite, characterized by a dispersion of pure ($<0.1\mu\text{m}$) niobium particles dispersed within a pure copper matrix [7]. This approach has the potential to produce high conductivity, high strength alloys in bulk forms, provided the microstructure is of sufficiently fine scale.

In this study, another PM technique, the rapid solidification of a gas atomized Cu-21.2 wt% Nb alloy, has been used as a method of producing alloy powder particles with a fine-scale microstructure. As will be shown, the microstructural features which characterize the rapidly solidified powder particles are much different from those in a conventionally cast counterpart. One significant observation to the present study is

that of Verhoeven et al. [8] who observed the appearance of niobium-rich multiphase spheroids in chill cast Cu-15wt%Nb and Cu-20wt%Nb alloys which had been contaminated with oxygen. Another observation by Verhoeven et al. [6], perhaps more pertinent to the study, is the observation of fine Nb-rich spheroids in thin, rapidly quenched splates (0.5mm) that was attributed to the onset of a metastable monotectic reaction which occurs in Cu-Nb alloys at high solidification rates. This suggests that it might be possible to induce a liquid phase separation reaction and subsequently solidify the Nb-rich liquid as discrete spheroids dispersed throughout a Cu-rich matrix. An examination of the copper-niobium equilibrium phase diagram shown in Fig. 1 supports this hypothesis; metastable miscibility gaps have been observed to occur in similar systems in which smooth, flat liquidus lines extend over a range of compositions [10-12]. Rather than stabilizing the miscibility gap with oxygen contamination, the present study utilizes high pressure gas atomization and the associated benefits of rapid solidification as a means of inducing metastable liquid phase separation and, subsequently, maintaining the inhomogeneity into the solid state. The microstructural evolution of the resulting Cu-21.2wt%Nb powder particles will be shown to depend on particle size and is analyzed in terms of the influence of atomization and rapid solidification on undercooling and the associated solidification sequence.

2. Experimental

2.1 High Pressure Inert Gas Atomization

Atomization of a copper - 21.2wt% niobium alloy was performed at the Ames Laboratory, USDOE, where a new high pressure gas atomizer has been designed and constructed. An HPGA atomizer* differs from other atomizers which are commercially used in that the intense gas shock effects induced by the special nozzle design and

* U.S. Patent 4,619,845

the elevated atomization gas pressures can produce a substantial yield of fine ($<10\mu\text{m}$) powders [13]. This process utilizes the high kinetic energy generated from the interaction of focused supersonic gas jets on a close-coupled melt stream to cause disintegration of the alloy into highly dispersed droplets of metal [14]; see Fig. 2. The overall design of the atomizer, as shown in Fig. 3, is also unique. It consists of a large upper chamber, in which induction melting of up to 5 kg of material is possible, a long, slender lower chamber, wherein atomization of the melt is performed, and a powder collection facility, which includes a tornado-type separator to remove and isolate the powder from the atomization gas stream. To reduce the risk of powder contamination, the entire system can be evacuated and subsequently backfilled with an ultra-high purity (UHP) inert gas prior to use. In addition, the powder collected from an experiment can be remotely isolated under UHP inert gas and removed to proper storage facilities without exposure to the environment.

In the present study, a Cu-Nb alloy was atomized using the high pressure inert gas atomizer described above. The initial charge consisted of a consumable arc melted ingot of Cu-19.6 wt.% Nb composition. The charge was heated and subsequently held for 5 minutes at 2000°C , which is approx. 270°C above the melting point of the alloy, in a molybdenum-based crucible under UHP argon at 1.1 atm. pressure. Atomization was accomplished using UHP argon gas at an inlet pressure of 1750 psi, which was previously determined to produce the optimum yield of fine powders [15]. The resulting Cu-Nb powder was isolated under UHP argon and subsequently transferred into a vacuum glove box for storage.

2.2 Material Characterization

Before any microstructural characterization could be performed, an ATM Sonic Sifter was used to classify the atomized powder into several specific size ranges. An ISI SX40A Scanning Electron Microscope (SEM) was used to study the powder

surface features as a function of powder particle size. Samples were prepared by suspending a small portion of powder in ultrapure trichlorotrifluoroethane, dispersing this slurry on an aluminum stub, vacuum drying, and then sputter depositing the surface with a thin layer of gold to improve secondary electron imaging.

To evaluate the microstructures of the individual powder particles, a multistep metallographic technique was developed. This involved suspending approximately 0.5 grams of each size class of powder particles in a small amount of epoxy, allowing this to cure, and then remounting this "minisample" in additional epoxy to produce a small area containing a high concentration of powder particles, which were well bonded together and supported by the additional epoxy. The cross-sections of the powders were exposed by first carefully grinding with 400 and 600 grit SiC paper and subsequently polishing with diamond compounds suspended in pure kerosene. The final polish consisted of 0.05 μ m alumina suspended in deionized water.

The amounts and morphologies of the various phases present within the microstructures of the powder samples were determined using a backscattered electron detector attached to the SEM described above. With proper image analysis, this technique permitted a determination of the amount of Nb-rich phases as a function of powder size. To study the size and morphologies of the Nb-rich second phases, a deep-etch technique was used to remove the Cu matrix prior to SEM observations with a secondary electron detector. This was accomplished by immersing the samples in a solution consisting of 30% H₃PO₄, 15% CH₃COOH, 10% HNO₃, and 45% ethyl alcohol for approximately 20 seconds, after which each was carefully rinsed with trichlorotrifluoroethane, vacuum dried, and finally sputter-coated with a thin layer of gold to enhance electron imaging.

3. Results

The atomization experiment produced approximately 1000 grams of powder smaller than 88 μ m (170 mesh) in diameter, with a size distribution as presented in Figure 4. The size distribution was determined by scanning electron microscopy (SEM) revealed that powder particles of diameters up to approximately 63 μ m had spherical shapes; see Fig. 5. Particles larger than 63 μ m tended to be irregular in shape. Excessive agglomeration of powder particles was not observed, although some attachment of small (0.5 to 1 micron) particles to larger ones is seen, arrowed 1 in Fig. 5.

A chemical analysis of a representative sample of the full size distribution of atomized powders, presented in Table I, indicated that the Nb content of the HPGA powder was 21.20 wt.% rather than 19.6 wt.% Nb, the nominal charge composition. Because of this result, the alloy is referred to, throughout this report, as Cu- 21.2 wt.% Nb. This apparent Nb enrichment of the alloy most probably resulted from selective vaporization of the Cu from the molten atomizer charge during the temperature excursion up to the pour temperature of 2000°C that was required for alloy homogenization and atomization superheat. The analysis also detected a Mo content of 1.80 wt.%. The apparent source of the Mo was a sluggish dissolution of the Mo-based crucible inner wall (increase in radius of about 1.3mm) that was noted after the atomization experiment. This residual Mo probably is present in the alloy powders in solid solution form within the Nb-rich phase and is not likely to significantly affect the phase relationships of Cu and Nb. An analysis of the residual gas content in the powders by a vacuum fusion technique detected an oxygen content of 290 ppm (wt.), as listed in Table 1. This purity level compares favorably with the results of Verhoeven, et al. [8] on bottom pour chill cast Cu-20 wt.% Nb ingots, where a variety of different refractory crucible materials were tested for residual oxygen contamination

properties. The best crucible material, Y_2O_3 , produced an ingot with an oxygen content of 180 ppm, converted to a wt.% basis.

As summarized in Table II, the microstructures generated during the HPGA of the Cu-Nb alloy depend on powder particle size. The "large" powder, classified herein as those particles between $45\mu\text{m}$ and $75\mu\text{m}$ in diameter, exhibited a microstructure which is typified by Fig. 6. The Nb-rich phase volume fraction was approximately 22%, as measured by quantitative metallography techniques. This measured volume fraction agrees well with the calculated value of Nb appeared as well formed, fine-scale dendrites (stalk diameters of 0.3 to $0.5\mu\text{m}$) distributed within the Cu matrix. It should be noted that essentially all of the Nb present in a Cu-21.2wt%Nb alloy is present as a Nb second phase since Cu and Nb have nearly complete mutual solid state solubility [9].

In contrast to the above, the microstructures of the "fine" powders, classified as those less than $15\mu\text{m}$ in diameter, consist primarily of a distribution of spheroidal particles together with a few dendrites distributed within the copper matrix; see Fig. 7. Within the fine powder particles, the volume fraction of the Nb-rich phase measured about 35% (10% dendrites + 25% spheres). This indicates that the spheroids are not pure niobium (assuming that the dendrites are nearly pure niobium). A cross-sectional view of the spheroids is shown in Fig. 7b and reveals that they are, in fact, multiphase. Backscatter SEM imaging in conjunction with EDS micro-analysis indicates that the spheroidal particles have Nb-rich shell, arrowed 1 in Fig. 7b, and an interior consisting of both Nb- and Cu-rich phases, arrowed 2 and 3, respectively. The significant amounts of Cu in the spheroidal particles results in the enhancement of the "second" phase volume fraction from $\approx 22\%$ in the large powder particles to $\approx 35\%$ in the fine particles. The diameter of the spheroid particles within the fine powders varied from <0.1 to $2.0\mu\text{m}$. In addition, a few small dendrites were observed at both the powder particle surface and randomly distributed within the interior.

The "medium" size powder particles, classified as those between 15 and 45 μm in diameter, possess microstructures as shown in Fig. 8. Within this powder size range, as particle size increases, the volume fraction of dendrites increase relative to the volume fraction of spheroids. As the dendrite volume fraction nears total dominance over the spheroids the overall volume fraction of the second phase(s) decreases toward 22%. As previously noted, this value compares favorably to the volume fraction of a pure second Nb second phase as predicted from the chemical analysis of the Nb in this alloy: 21.9 vol%.

4. Discussion

The microstructural observations indicate that rapid solidification via high pressure gas atomization of a Cu-21.2wt%Nb alloy produces powders whose microstructures vary with particle size. Fine powders (<15 μm in dia.) consist primarily of Nb-rich spheroids dispersed within a Cu matrix. The microstructure of large powders (>45 μm in dia.) contains the Nb phase in well-formed dendrites within a Cu matrix. Medium sized powders (15 to 45 μm in dia.) have a mixed spheroid/dendrite Nb phase morphology with the Cu matrix phase. In order to interpret the observation of two distinct particle microstructure types in small and large powder sizes and of a mixed morphology in medium powder sizes, the impact of undercooling and the evolution of rapid solidification in gas atomized powders must be examined.

The formation of Nb-rich spheroids within the fine powders suggests that a liquid-liquid phase separation had occurred during cooling of the atomized droplets, before solidification was initiated. As the literature indicates, a liquid-liquid miscibility gap may be an equilibrium feature of the Cu-O-Nb ternary system, that is accessed by alloy liquid undercooling, prior to a solidification reaction. Verhoeven and Gibson [8] report that the typical solidification morphology of a Cu-20 wt.% Nb alloy casting consists of well-formed Nb dendrites in a Cu matrix for oxygen concentrations of less than 544

ppm (wt.). A spherical Nb-rich phase morphology was observed for oxygen contents greater than about 544 ppm. The authors concluded that for high oxygen contents an equilibrium liquid-liquid miscibility gap could be stabilized. This shift in phase equilibria behavior was applied to explain an earlier Cu-Nb equilibrium phase diagram study [16] that had reported a monotectic reaction in this system, i.e., the melting environment used earlier had provided an elevated level of oxygen contamination. It should be noted that the oxygen content of the HPGA powder (290 ppm) compares favorably to the lowest reported level (180 ppm) for a chill cast ingot [8], in spite of the much greater surface area per gram of the powder. The low oxygen content of the as-atomized powder coupled with the observation of well-formed Nb dendrites in the large powders ($> 45\mu\text{m}$) strongly indicates that the oxygen content of the powders was not sufficient to stabilize an equilibrium ternary Cu-O-Nb monotectic reaction.

Previous studies also have found the microstructures of gas-atomized powders to be a strong function of particle size [17], especially if fine ($<10\ \mu\text{m}$ dia.) powders were included in the investigation. A shift in solidification reaction path with a reduction in particle size implied by the observation of different particle solidification microstructure types was attributed to the onset of high undercooling behavior [17]. Specifically, Anderson and Kemppainen [17] demonstrated that $<5\mu\text{m}$ dia. inert gas-atomized powders of Cu-Si and Cu-Al alloys could experience high undercoolings of $0.23T_m$ and $0.28T_m$, respectively. Such high undercooling behavior is promoted by a "mote isolation" effect [18] which occurs in a finely divided melt and by the clean, "containerless" conditions of solidification during free fall in an atomization chamber containing an inert atmosphere. The mechanism of the mote isolation effect begins from the assumption that a certain population of potent heterogeneous nucleation catalysts, or motes, exists within a given volume of an alloy melt. Upon atomization of the melt into a collection of fine droplets, the probability that any one of the droplets

contains a heterogeneous crystal nucleation site depends on the random distribution of the motes within these isolated liquid droplets, where the mote-free fraction of powder particles, X , can be estimated by:

$$X = \exp(-Mv) \quad [1]$$

where M is the total mote concentration in the melt and v is the volume of each resulting droplet. On cooling, a large value of X , which is enhanced as particle size is reduced, indicates that a large fraction of droplets are mote-free, promoting rapid solidification at high undercoolings. This hypothesis is valid only if the surfaces of the isolated liquid droplets, e.g., an inert gas-atomized droplet spray during free fall, are maintained in a clean (low catalytic activity) condition. In other words, the gas environment must be controlled to inhibit growth of a thick crystalline oxide layer, for example, on the powder surfaces to minimize their possible catalytic influence on crystal nucleation.

The high pressure gas atomization process, used to produce the Cu-Nb powder, appears to satisfy both of the criteria for encouraging high undercooling. Namely, the particle size distribution of the powder yield, shown in Figure 4, indicates a high degree of droplet dispersal, i.e., mote isolation, and the low oxygen content and spherical shape of the powders, summarized in Table I and Figure 5, indicates the clean conditions of droplet freefall during the process i.e., containerless solidification. Therefore, a metastable liquid spinodal was likely to have caused the spherical Nb phase morphology development that was observed in the fine ($<15\mu\text{m}$) Cu-Nb alloy powders, promoted by a high undercooling level. A schematic of the metastable miscibility gap and its probable location on the equilibrium Cu-Nb phase diagram is given in Figure 9.

The solidification morphology of the Nb phase in large ($>45\mu\text{m}$ in dia) gas-atomized powders, well-formed, finely-spaced dendrites (0.1 to $0.5\mu\text{m}$ arm dia.), appears to result from a well understood solidification process extended to include the rapid quenching conditions of a high pressure gas atomizer. In other words, constitutional supercooling of the Cu-Nb alloy appears to promote the level of morphological instability necessary to cause rapid dendritic growth within the large alloy droplets during solidification. The high probability (essentially certain) of mote contamination within these large droplets precludes the development of high liquid undercoolings but the rapid gas cooling (about 10^5 °C/sec.) of the droplet surfaces allows sufficient interfacial supercooling for very rapid dendritic growth to occur. Numerous observations of this level of refinement in dendrite arm dimensions have been made in comparisons of ingot castings with rapidly quenched ribbons and gas atomized alloy powders [19]. In fact, this scaling "law" forms part of the basis for conventional estimates of the cooling rates of numerous rapid solidification approaches.

The medium size powder particles (15 to $45\mu\text{m}$ in dia.) contain spheroids and dendrites of the Nb phase suggesting that the solidification reaction path in these Cu-Nb droplets depends on both undercooling and rapid growth. A kinetic competition appears to have been established between liquid-liquid phase separation and nucleation and growth of Nb dendrites. Evidence for this competition is found in the typical locations of the dendrites within the particle microstructure, both randomly oriented within the particle interior and attached radially to particle exterior surfaces. It is likely that the random dendrites nucleated on Nb-rich liquid pockets because of the enhanced supersaturation of these regions. Also, the radially oriented dendrites may have nucleated on the droplet surface due to various favorable influences and apparently grew from the droplet exterior surface inward because of the radially outward heat flow direction that operates in spherical gas atomized particles.

Metallographic observations suggest that the fraction of dendritic Nb phase in the mixed particle microstructure is reduced as the particle size is reduced. Thus, it seems that the nucleation and growth of Nb dendrites interrupts the full development of the spheroidal morphology because the undercooling level of these droplets is not sufficient to permit complete solidification of the particles immediately after liquid-liquid phase separation.

As the droplet size is reduced further (below $15\mu\text{m}$), the effects of the kinetic competition between liquid phase separation and niobium solidification is reduced. High levels of undercooling become almost certain as sites, or rather motes, for nucleation of solid niobium diminish. The microstructural evolution is then controlled by the limits set forth by the metastable miscibility gap, Figure 9, rather than by the equilibrium phase diagram. Figure 10, backscatter SEM images of very fine ($<10\mu\text{m}$) powder particles, confirm this supposition that liquid phase separation dominates these microstructures. As is shown, the microstructure consists of a high percentage ($>25\%$) of spheroids with still a certain amount of dendrites (5-10%) present, the lower limit of which is controlled by the solubility limit of niobium in the copper-rich liquid as defined by the metastable phase diagram.

The preceding analysis may be summarized with the schematic illustrations in Figure 11, which depicts the sequence of events that occur along the solidification reaction path for a $<15\mu\text{m}$ (fine scale) droplet from time, t_0 , of droplet formation to the time, t_4 , of final particle solidification. At time = t_0 , atomization of the melt into various size droplets of the Cu-21.2wt%Nb liquid occurs. At $t_1 > t_0$, the smallest droplets ($<15\mu\text{m}$) which are likely to be mote-free, undercool to a degree that Nb-rich liquid separates into small spherical pools throughout a Cu-rich liquid matrix. This occurs by either nucleation and growth and/or by spinodal decomposition [20]. We estimate that at temperatures near solidification, the Nb-rich liquid has a compositions of roughly

Cu-50wt%Nb.* As discussed in detail elsewhere [8], thermodynamics governing this system (under HPGA conditions) may be such that, despite a larger free energy of formation to form solid Nb, liquid phase separation occurs because of a smaller nucleation barrier. This is revealed by comparing the surface energies of liquid/liquid and liquid/solid interfaces where, typically, $\gamma_{L_1L_2}$ is much smaller than either γ_{SL_1} or γ_{SL_2} [21]. At some point, schematically represented as $t_2 > t_1$ on Fig. 11, heterogeneous nucleation of solid Nb at the L_1/L_2 interface within the fine droplets commences, as the large amount of undercooling achieved by the droplet overcomes the activation barrier to form solid Nb. The spherical nature of this dispersion suggests that it had formed before the matrix had solidified while its fine scale suggests that the cooling rate had been effective in preventing coalescence. At $t_3 > t_2$, recalescence, in addition to the isolation effect of the continuous shell, causes the interior of the Nb-rich "spheroids" to slowly solidify along an equilibrium path. This results in the two phase lamellar microstructure of the spherical particles; as shown in Fig. 7b. In addition, the latent heat generated by the formation and subsequent solidification of the Nb-rich spheroids slows the cooling rate of the Cu-rich liquid matrix as it begins to solidify. A few, small niobium dendrites will thus nucleate and grow as the copper-rich liquid follows the equilibrium liquidus, rejecting solute as the temperature decreases. At $t_4 > t_3$, the final solidification event occurs as the nearly pure Cu matrix solidifies around both the spheroidal and dendritic particles. For larger droplets, the solidification sequence would be similar, with the exception that liquid phase separation, controlled by the metastable diagram, would be progressively replaced by nucleation and growth of niobium dendrites, following the limits set forth by the equilibrium phase diagram.

From the preceding discussion, it has been made clear that the morphology and volume fraction of the niobium-rich second phase is dependent on the powder size

* This is based on the assumption that the Nb-rich dendrites are pure Nb and that 35 vol% of (spheres + dendrites) is achieved by spheres of composition Cu-50 wt% Nb in this Cu-21.2 wt% Nb alloy.

produced, derived from the degree of metastability attained prior to solidification. From comparisons to previous studies, it is also evident that the amount of oxygen present during the initial stages of solidification [8] also influence the resulting microstructure. Additional atomization experiments are required, involving various binary compositions, particle size distributions and oxygen levels, to yield a more complete description of the metastable limits of the copper- niobium system. This information, relating microstructure to processing history, could then be used to successfully control the microstructure and subsequent properties of high conductivity, high strength alloys produced from such powder.

5. Summary

High pressure gas atomization has been used to rapidly solidify Cu-21.2wt%Nb powder particles, the microstructures of which vary with particle size. Fine-scale particles (<15 μ m) have microstructures consisting of a continuous Cu matrix and a predominance of multiphase Nb-rich spheroids and a few nearly pure Nb dendrites. Formation of Nb-rich multiphase spheroids indicates that a liquid phase separation has occurred; this is attributed to a combination of significant undercooling and rapid cooling within the molten droplet solidification. As a result of such a solidification reaction, the volume fraction of 'second-phase' particles (spheroids plus dendrites) approaches 35%. As powder size increases and undercooling plus cooling rate decreases, the multiphase spheroids are replaced by a nearly pure Nb second phase in the form of dendrites. In this case, the volume fraction of second phase is that expected if it is pure Nb: 22.5 vol%. The microstructure of the powders may be understood in terms of both the amount of undercooling and cooling rate available to each particle.

Acknowledgements

Valuable technical discussions with Professor J. Verhoeven are greatly appreciated. In addition, the authors are grateful to Robert Terpstra for his assistance with the atomization experiments. The authors wish also to acknowledge the support of both the Office of Naval Research (The Pennsylvania State University) and the Department of Energy (Ames Laboratory).

References

1. C. C. Tsuei and L. R. Newkirk, *J. Mat. Sci.*, **8** (1973) 1307.
2. C. C. Tsuei, *J. Appl. Phys.*, **45** (1974) 1385.
3. G. Frommeyer and G. Wassermann, *Acta Metall.*, **23** (1975) 1353.
4. J. Bevek, J. P. Harbison, and J. L. Bell, *J. Appl. Phys.*, **49** (1978) 6031.
5. P. D. Krotz, "Mechanical Properties of Cu-20%Nb and Cu-20%Ta in situ Composites Between 22 and 600°C", Masters Thesis, Iowa State University (1986).
6. J. D. Verhoeven, W. A. Spitzig, F. A. Schmidt, P. D. Krotz, and E. D. Gibson, *J. Mat. Sci.*, **24** (1989) 1015.
7. M. A. Morris and D. G. Morris, *Mat. Sci. Eng.*, **A111** (1989) 115.
8. J. D. Verhoeven and E. D. Gibson, *J. Mat. Sci.*, **13** (1978) 1576.
9. D.J. Chakrabarti and D.E. Laughlin, *Bulletin of Alloy Phase Diagrams*, **2**, 4 (1982) 455.
10. S. P. Elder, A. Munitz, and G. J. Abbaschian, *Mat. Eng. Forum*, **50** (1989) 137.
11. S. K. Dhua, S. Raju, and K. Chattopadhyay, *Met. Trans. A*, **18A** (1987) 1131.
12. J. H. Perepezko and W. J. Boettinger, *MRS Symp. on Alloy Phase Diagrams*, L. H. Bennett, T. B. Massalski, and B. C. Giessen eds., Vol. 19, p. 223, Elsevier, North-Holland (1983).
13. I. E. Anderson and B. B. Rath, in *Rapidly Solidified Crystalline Alloys*, S. K. Das, B. H. Kear, and C. M. Adam eds., p. 219, The Metallurgical Society of AIME, Warrendale, PA, (1985).
14. I. E. Anderson and R. S. Figliola, in *Modern Developments in Powder Metallurgy*, Vol. 20, p. 205 (1988).
15. I. E. Anderson, K. L. Zeik, and R. P. Terpstra, Unpublished Work.
16. I.A. Popov and N.V. Shiryayeva, *Russ. J. Inorg. Chem.*, **6**, (1961) 1184.
17. I. E. Anderson and M. P. Kemppainen, in *Undercooled Alloy Phases*, E.W. Collings and C.C. Koch eds., The Metallurgical Society of AIME, Warrendale, PA, (1986).

18. D. Turnbull, in Undercooled Alloy Phases, E.W. Collings and C.C. Koch eds., The Metallurgical Society of AIME, Warrendale, PA, (1986) 3.
19. M.C. Flemings, Solidification Processing, McGraw-Hill, New York, p. 146 (1974).
20. S.P. Elder, A. Munitz, and G.J. Abbaschian, *Mat. Sci. Forum*, **50** (1989) 137.
21. B. Derby and J. J. Favier, *Acta Metall.*, **31**, 7, (1983) 1123.

TABLE 1. Chemical analysis of the atomized Cu-Nb alloy.

Element	Percent by wt.
Cu	76.46
Nb	21.20
Mo	1.80
C	120 ppm
O	290 ppm
H	45 ppm
N	43 ppm

TABLE 2. Summary of the microstructural characterization of HPGA Cu-21.2 wt%Nb as a function of powder size.

Powder Size (μm)	Powder Shape	MICROSTRUCTURE			
		Second Phase Morphology	Second Phase Vol. Fract.	Spheroid Size (μm)	Dendrite Stalk Diameter (μm)
- 15	spherical	Mainly Spheroidal	35%	<0.1 - 1.5	0.2 - 0.3
- 45 + 15	spherical	Spheroids/Dendrites	\approx 25%	<0.1 - 2.0	0.2 - 0.3
- 63 + 45	spherical	Dendrites	22.5%	NA	0.3 - 0.5
- 90 + 75	some irregular	Dendrites	22.5%	NA	0.3 - 0.6

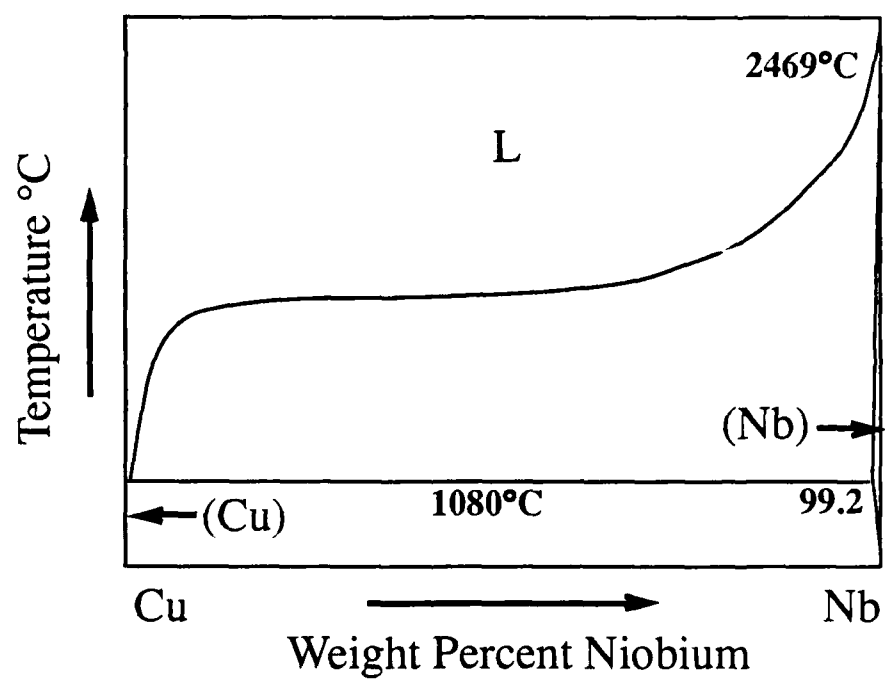


Figure 1. The Copper-Niobium equilibrium phase diagram, after Chakrabarti et al.[9].

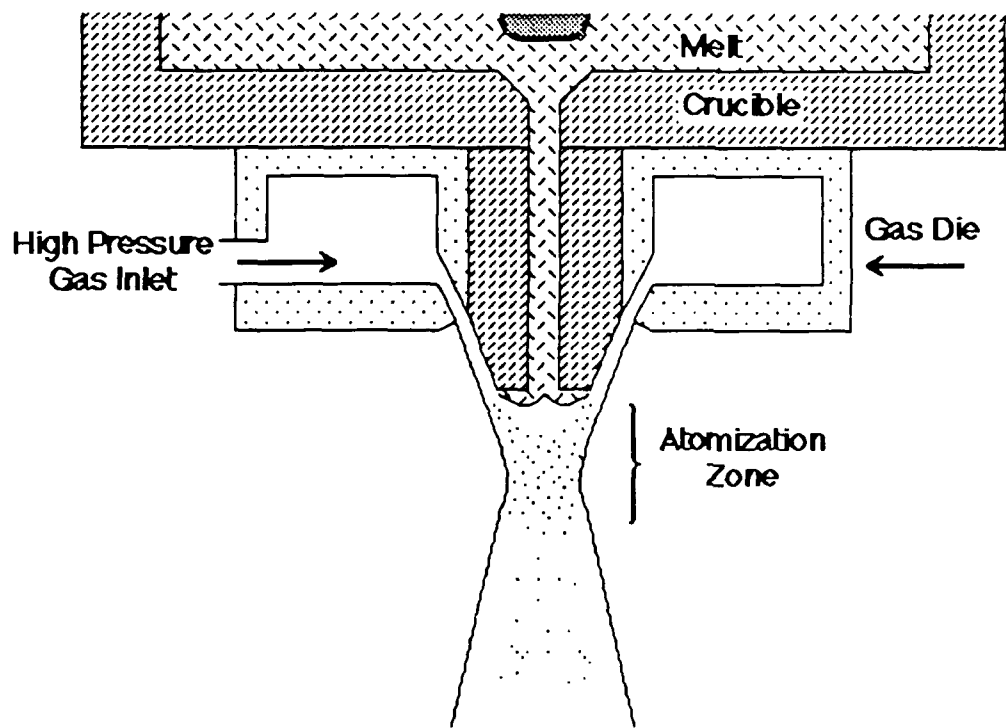


Figure 2. Schematic representation of the melt feed and nozzle configurations for the Ames Lab high pressure gas atomizer.

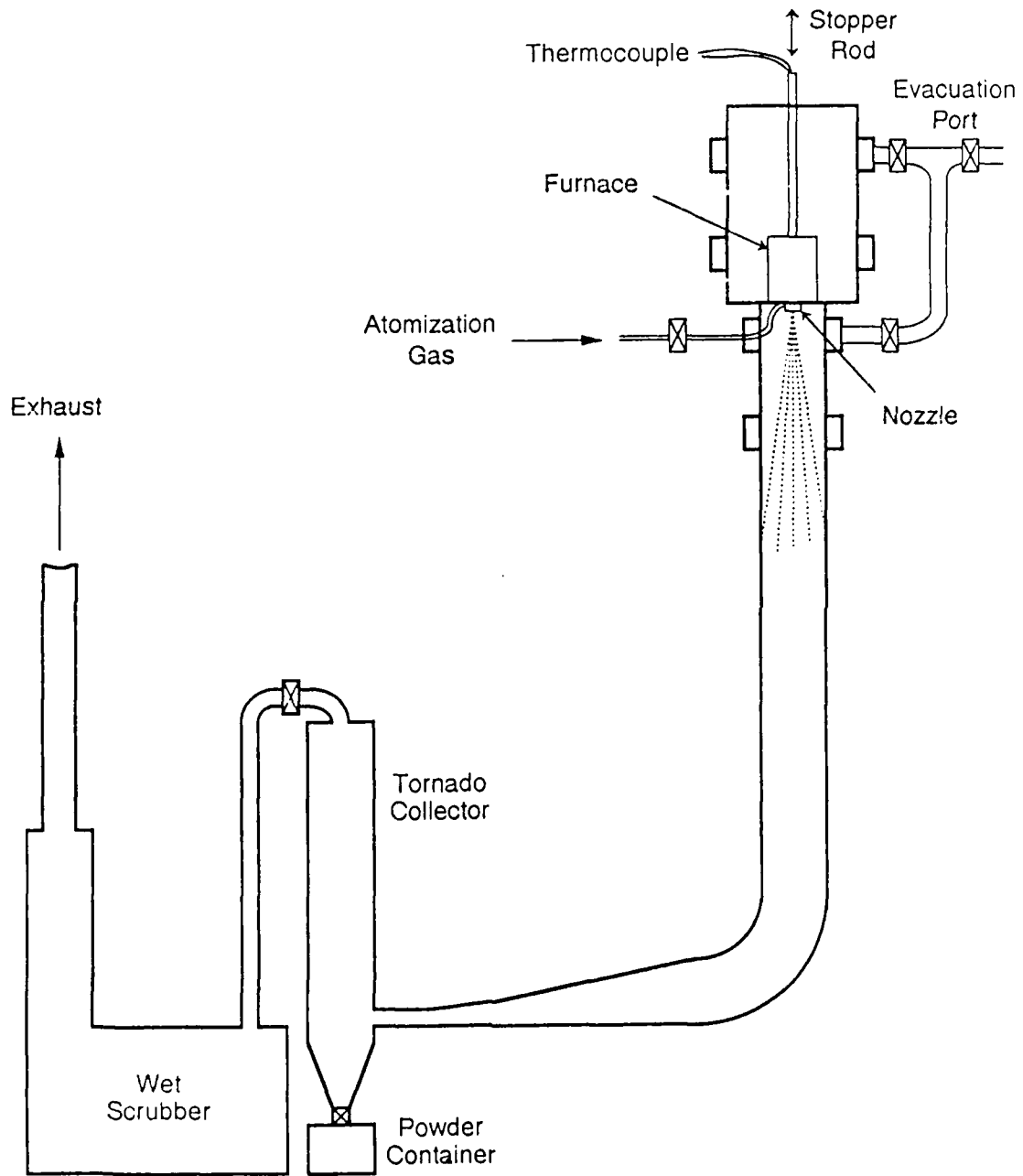


Figure 3. Schematic representation of the Ames Laboratory High Pressure Gas Atomizer (HPGA).

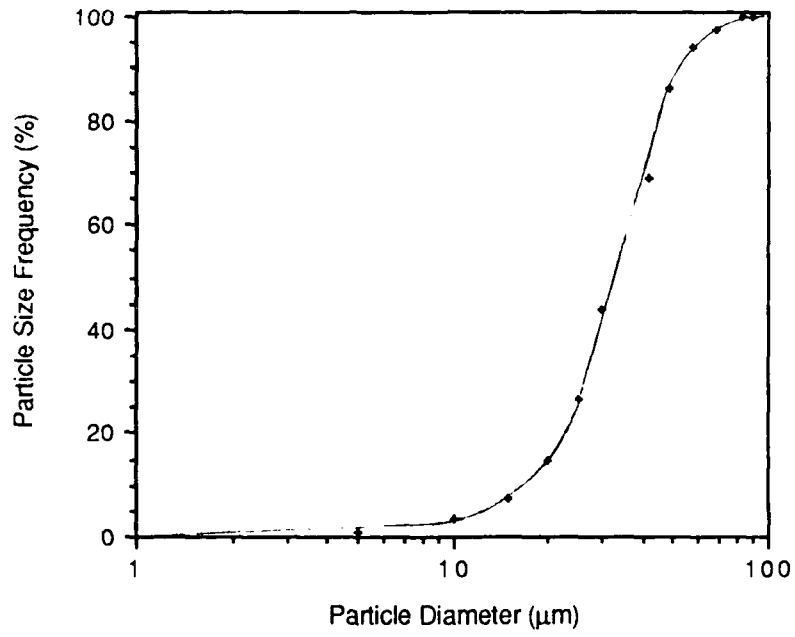


Figure 4. Particle size analysis from the HPGA of Cu - 22.3vol% Nb alloy

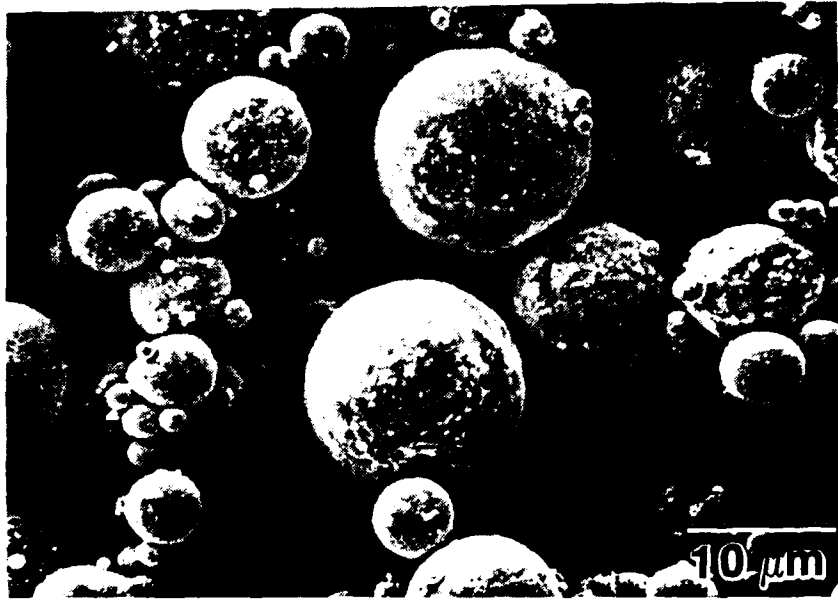


Figure 5. Scanning electron micrograph of the as-atomized powder surfaces.

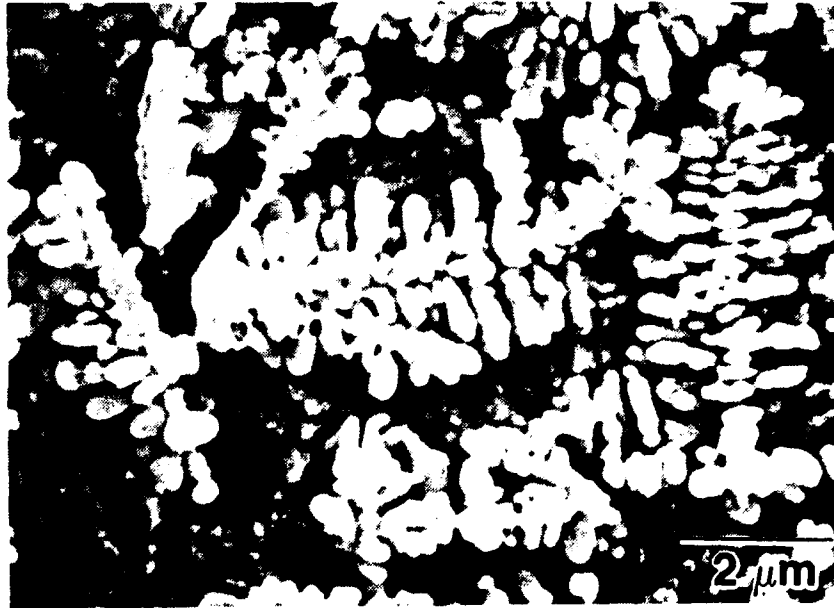


Figure 6. Scanning electron micrograph of the microstructure of a single, large (53 μm) powder particle containing a distribution of niobium dendrites. The copper matrix has been chemically removed.

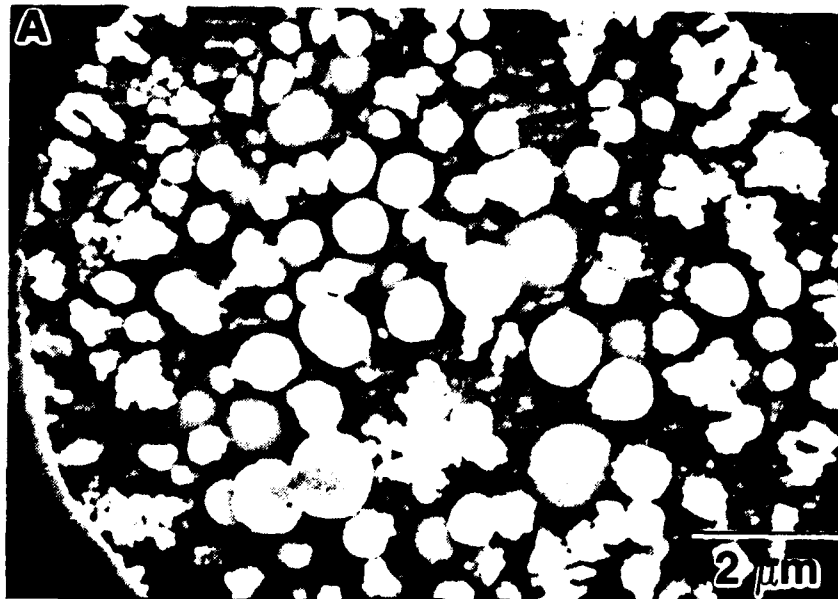


Figure 7. Scanning electron micrograph of a) the microstructure of a single, small (10 μm) powder particle and b) a cross-section view of one single spheroid contained within this microstructure.

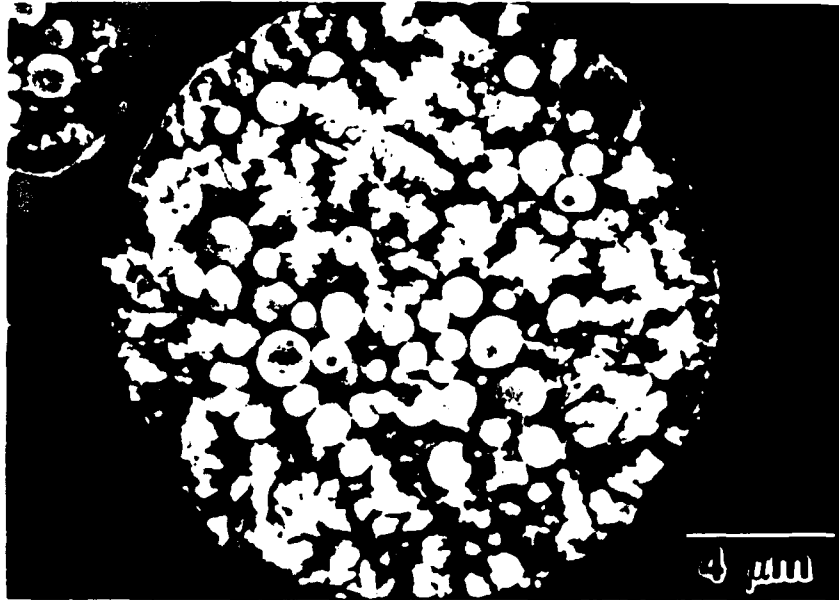


Figure 8 Scanning electron micrograph of the microstructure of a medium (20 μ m) size powder particle which contains large amounts of both niobium-rich spheroids and dendrites

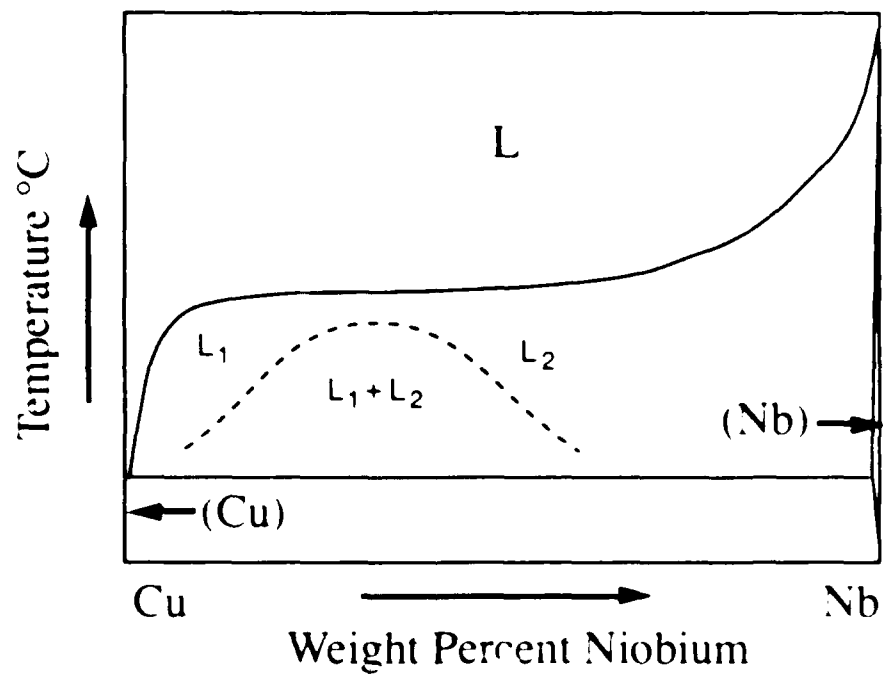


Figure 9. Schematic of the metastable miscibility gap (dashed lines) superimposed under the equilibrium phase diagram for the Cu-Nb alloy system.

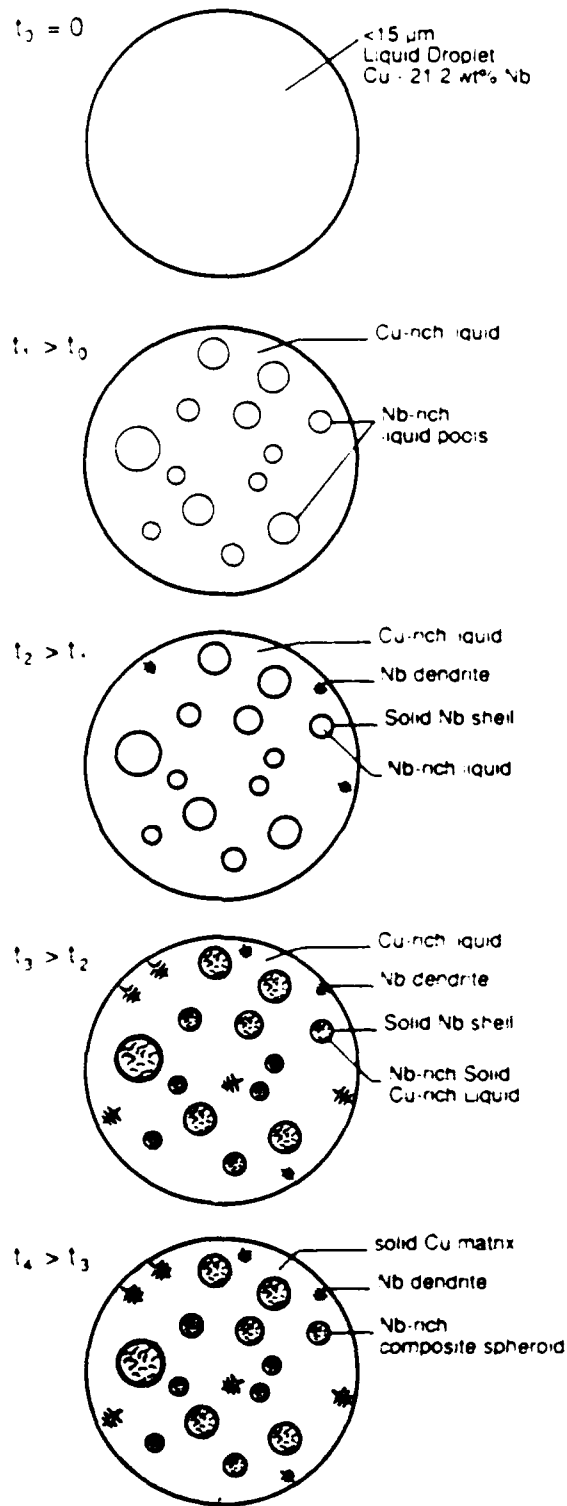


Figure 11. Schematic representation of the solidification path experienced by a small ($<15\ \mu\text{m}$) Cu-Nb droplet formed during atomization.

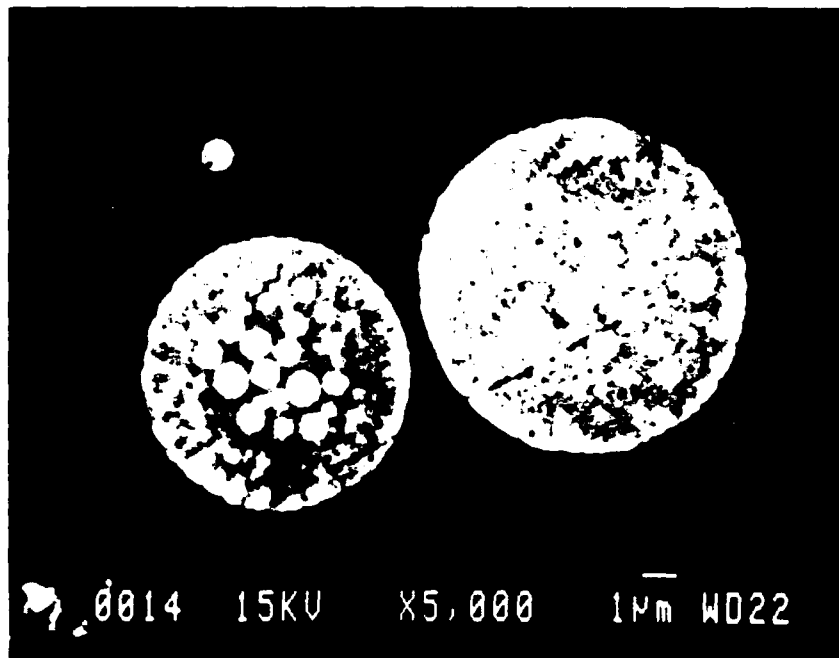


Figure 10. Backscatter electron micrograph of the microstructure of fine scale ($<15\mu\text{m}$) powder particles. Note the large amount of spheroidal second phase particles, arrowed 1.